

# Nonlinear Steady Incompressible Lifting-Surface Analysis with Wake Roll-Up

Emil O. Suciu\* and Luigi Morino†  
Boston University, Boston, Mass.

The problem of lifting surfaces in steady incompressible flow is considered. The problem is formulated in terms of an integral equation relating the potential discontinuity  $\Delta\phi$  on wing and wake to the normal derivative of the potential (normal wash) on the lifting surface. The integral equation is approximated by a system of linear algebraic equations obtained by dividing the surfaces into small quadrilateral elements and by assuming the potential discontinuity and the normal wash to be constant within each element. The wake geometry is obtained through iteration by satisfying the condition that the velocity be tangent to the surface of the wake and that  $\Delta\phi$  be constant along the streamlines. Numerical results are in good agreement with existing ones.

## Nomenclature

$a_k$	= base vectors
$A_{hk}$	= Eq. (12)
$b$	= span
$c_l$	= lift distribution coefficient $c_{pl} - c_{pu}$
$c$	= chord
$D$	= doublet strength
$D_k$	= value of $D$ at centroid of element $\Sigma_k$
$\ell_w$	= length of wake
$n$	= normal to $\Sigma$
$N_x, N_y$	= number of elements in $x, y$ directions
$P$	= point of the surface $\Sigma$
$P^*$	= control point, $(x^*, y^*, z^*)$
$r$	= Eq. (2)
$x, y, z$	= space coordinates
$U_\infty$	= freestream velocity
$V$	= velocity vector
$V_{hk}$	= Eq. (11)
$\alpha$	= angle of attack
$\Sigma$	= surface of wing and wake
$\Sigma_k$	= surface element
$\Sigma_w$	= surface of wake
$\Phi$	= velocity potential
$\phi$	= perturbation velocity potential, $\Phi/U_\infty - x$
$\phi_k$	= values of $\phi$ at centroid of element $\Sigma_k$
$AR$	= aspect ratio
$\Delta\phi$	= $\phi_u - \phi_l$
$\nabla^*$	= gradient in $x^*, y^*, z^*$ space

## I. Introduction

THIS paper deals with the analysis of the wake roll-up for lifting surfaces. The ultimate goal of the present study is the accurate evaluation of the effect of the wake roll-up on the pressure distribution on interfering surfaces (such as wing and tail) and/or complex aircraft configurations (such as the space shuttle). Therefore the emphasis of the paper is on the roll-up region of the wake (near-field wake), although the method is applicable to the whole inviscid roll-up region.

The interest in the phenomenon of wake roll-up has been renewed by the introduction, a few years ago, of the wide-

Received July 16, 1976; revision received Sept. 27, 1976. This work was supported by NASA Langley Research Center under NASA Grant NGR 22-004-030. The authors wish to express their appreciation to Dr. E. Carson Yates Jr., monitor of the program, for stimulating their interest in this research area and for his suggestions and comments made in connection with this work.

Index category: Jets, Wakes, and Viscid-Inviscid Flow Interactions.

\*Research Assistant. Student Member AIAA.

†Director, Computational Continuum Mechanics Program. Member AIAA.

body aircraft. The phenomenon has been the subject of both experimental and theoretical investigations. An excellent survey of the work performed on the wake roll-up can be found in Ref. 1, where it is observed that most theoretical investigations deal with the problem of the far-field wake. In such case the wake is accurately modeled as a two-dimensional array of point vortices. A set of time-dependent differential equations describe the motion of the vortices in the Trefftz plane. The loading of the wing is assumed to be known (usually elliptical) and not influenced by the roll-up process. The solution of these equations was found to be unstable.<sup>2</sup> Some correction factors were introduced (see for example the artificial viscosity method of Ref. 3), but, even though the solution looks more "reasonable," these factors introduce other errors, the magnitude of which is difficult to estimate.<sup>1</sup> On the other hand, according to Ref. 1, relatively little work is being done on the problem of interest here. Efforts to include the effect of the roll-up of the wake on the lift distribution are given in Refs. 4 and 5. However "a general method for finding the complete wake is not yet available."<sup>1</sup>

The present paper introduces a conceptually new method for analyzing the phenomenon of the wake roll-up. The method is general and can be used to find the complete wake and to evaluate the effect of the wake roll-up on the pressure distribution, although the preliminary results presented to validate the general method are limited to simple configurations. In this method the wake is represented not as a vortex array but as a sheet of doublets. The paper uses the exact nonlinear three-dimensional integral formulation for lifting-surfaces in steady, incompressible, inviscid, irrotational flow, presented in Ref. 6. The formulation is given in terms of the perturbation velocity potential. The main advantage of the method is that by using a doublet sheet (instead of an equivalent vortex sheet) the method may be easily extended to steady and unsteady, subsonic and supersonic flows around complex aircraft configurations by using the formulation of Refs. 7 and 8.

The exact nonlinear equations are approximated with a discrete formulation based upon the finite-element technique. The only approximations are numerical. No small-perturbation assumption is invoked. The surfaces of the wing and of the wake (initially assumed flat) are divided into a number of small quadrilateral surface elements with  $\Delta\phi$  constant within each element. The rolled-up wake is obtained through a process of iteration.

## II. Lifting-Surface Theory

For a lifting surface, the perturbation velocity potential is given by the following integral expression (see for instance

Ref. 6)

$$\phi(P_*) = \iint_{\Sigma} D \frac{\partial}{\partial n} \left( \frac{1}{r} \right) d\Sigma \quad (1)$$

where  $\Sigma$  extends over the lifting surface and its wake,  $n$  is the upper normal,

$$r = [(x - x_*)^2 + (y - y_*)^2 + (z - z_*)^2]^{1/2} \quad (2)$$

( $x, y, z$  are the coordinates of the point on  $\Sigma$ ) and

$$D = \frac{\phi_u - \phi_l}{4\pi} \quad (3)$$

(the subscripts  $u$  and  $l$  stand for upper and lower surfaces, respectively). The boundary condition on the lifting surface is that the normal component of the velocity is zero. Formulated in terms of the perturbation velocity potential, the boundary condition becomes

$$\frac{\partial \phi}{\partial n} = -i \cdot n = -n_x \quad (4)$$

Using Eqs. (4) and (1), the following integral equation for  $\phi$  results

$$\frac{\partial \phi}{\partial n_*} = \iint_{\Sigma} D \frac{\partial^2}{\partial n_* \partial n} \left( \frac{1}{r} \right) d\Sigma \quad (5)$$

where  $\partial \phi / \partial n_*$  (the subscript denotes the control point) is known and given by Eq. (4).

The velocity is obtained by taking the gradient of Eq. (1). The pressure distribution coefficient is obtained from Bernoulli's Theorem. In particular, on the lifting surface, the lift distribution coefficient is evaluated as<sup>6</sup>

$$c_l = (2i + \nabla \phi_u + \nabla \phi_l) \cdot \nabla (\phi_u - \phi_l) \quad (6)$$

Finally, on the wake the following conditions must be satisfied: the velocity is tangent to the surface of the wake (i.e., the wake is composed of streamlines) and  $D$  is constant along the streamlines and equal to its value at the point of the trailing edge from which the streamline emanates: the condition that no pressure discontinuity exists across the wake is automatically satisfied.<sup>6</sup>

It should be emphasized that the preceding nonlinear formulation is exact. In particular no small-perturbation assumption is invoked in the boundary condition Eq. (4) or in the expression for the lift distribution coefficient, Eq. (6), or in the boundary conditions on the wake surface.

### III. Numerical Formulation

Next consider the numerical formulation. The lifting surface and the wake are divided into small surface elements  $\sigma_k$ . Assume that the value of  $D$  is constant within each element, say equal to  $D_k$  (unknown) at the centroid of the element  $\sigma_k$ . If we impose that the boundary condition, Eq. (4), be satisfied at the centroids  $P_h$  of the surface elements  $\sigma_h$  the following system of algebraic equations is obtained

$$[A_{hk}] \{D_k\} = \{B_h\} \quad (7)$$

with

$$B_h = \left( \frac{\partial \phi}{\partial n} \right) \Big|_{P_* = P_h} \quad (8)$$

and

$$A_{hk} = \left[ \iint_{\sigma_k} \frac{\partial^2}{\partial n \partial n_*} \left( \frac{1}{r} \right) d\sigma_k \right]_{P_* = P_h} \quad (9)$$

where for wing surface elements in contact with the wake  $\sigma'_k$  is equal to  $\sigma_k$  plus the wake strip emanating from  $\sigma_k$ , whereas  $\sigma'_k = \sigma_k$  otherwise.

In view of the Kutta condition, in deriving Eq. (7), the values of  $D_{TE}$  are approximated with the values of  $D$  at the centroids of the elements adjacent to the trailing edge.

The velocity at any point  $P_h$ , the field is obtained according to

$$V_h = U_{\infty} i + \sum_k D_k V_{hk} \quad (10)$$

with

$$V_{hk} = \left[ \nabla \cdot \iint_{\sigma'_k} \frac{\partial}{\partial n} \left( \frac{1}{r} \right) d\sigma'_k \right]_{P_* = P_h} \quad (11)$$

Note that, by definition,

$$A_{hk} \equiv n_h \cdot V_{hk} \quad (12)$$

If the surface elements are approximated by quadrilateral hyperboloidal elements passing through the four corner points<sup>7</sup> the integrals can be evaluated analytically,<sup>9</sup> as indicated in Appendix A. The integral over the wake strip is also evaluated by dividing the strip into quadrilateral hyperboloidal elements.

The iteration scheme used for obtaining the rolled-up wake geometry is based on the condition that the wake streamlines should be tangent to the velocity vector. Compute the doublet strength distribution at the centroids of the elements. Then calculate the velocity vector on the wake, at the corners of the surface elements. Align segments of the wake streamlines with the velocity vector evaluated at the upstream segment extremity. For example, consider two successive points along a wake streamline,  $P_i$  and  $P_{i+1}$ . The position of the point  $P_{i+1}$  is modified as follows

$$P_{i+1} = P_i + \Delta P \quad (13)$$

where

$$\Delta P = V_i |\Delta P| / |V_i| \quad (14)$$

$|\Delta P|$  is the original distance between the points  $P_i$  and  $P_{i+1}$  and  $V_i$  is the velocity vector at  $P_i$ . After the evaluation of the velocity at one point of the wake, the geometry of the wake is immediately modified before evaluating the velocity at the next point. then the doublet strength distribution is calculated again (there is a very small change from the preceding distribution, due to the new wake geometry), then the wake velocities and geometry are recalculated. The process is repeated until the difference between successive wake geometries becomes sufficiently small, thus indicating that convergence is attained (or the fact that the wake streamlines are indeed tangent to the velocity vector). In order to achieve savings of computation time, the computer program implementing the iteration scheme has some special features. First, since  $\Delta \phi$  changes very slightly from iteration to iteration, it is evaluated only every fifth iteration. Second, if the change in position of a point is less than  $10^{-4}c$ , the evaluation is skipped for the next iteration at that point. A final "complete" iteration is included in order to verify that convergence has been attained. Next consider the evaluation of  $c_l$ , given by Eq. (6). The average velocity,  $\nabla (\phi_u + \phi_l)/2$  is calculated by using Eqs. (10) and (11); however, the contribution of the surface element at which the coefficient is calculated is skipped since that element contributes only to the discontinuity on  $V$ . The term,  $\nabla (\phi_u - \phi_l)$ , is calculated from  $D$  by using finite differences.<sup>6</sup>

### IV. Numerical Results

The lifting surface formulation described in Section II was incorporated in the computer program ILSA (Incompressible

Lifting Surface Aerodynamics). All the results presented here were obtained with this program and are for rectangular lifting surfaces in steady incompressible flow.

The initially straight-wake geometry is automatically generated. The lengths of the wake elements increase with the distance from the wing trailing edge, following a quadratic law. For all the results presented here the iterative scheme is converged (typically after five iterations for the fifth figure).<sup>6</sup> All the figures show results for the semispan of the wings, with the center streamline being along the wing centerline and the outer streamline starting at the wingtip. A number of parameters define the type of the problem:  $c$  is the chord and  $b$  is the span of the wing, oriented along  $x$  and  $y$ , respectively;  $N_x$  and  $N_y$  are the numbers of surface elements on the right-hand side of the lifting surface in the  $x$  and  $y$  directions, respectively;  $\ell_w$  is the total length of the wake, not counting the last element, which equals one hundred times  $\ell_w$ ;  $N_w$  is the number of wake elements (except for the last one), along the  $x$  direction.

Figures 1-3 present a convergence analysis for a rectangular planar lifting surface of aspect ratio  $AR = 8$ , at an angle of attack  $\alpha = 5^\circ$ . The parameters which affect the convergence are the numbers of elements on the surface,  $N_x$  and  $N_y$  (in  $x$  and  $y$  directions, respectively), the length  $\ell_w$  of the wake (except for the last long element) and the number  $N_w$  of elements on the wake (except for the last one). The effect of  $N_x$  on convergence is negligible and  $N_x = 4$  was found to be adequate to give accurate results without excessive computer time. In addition, adding wake elements (and therefore increasing the length  $\ell_w$ ) has almost no effect on the convergence of the preceding wake elements. Therefore all the results in Figs. 1-3 are obtained with  $N_x = 4$  and  $\ell_w/c = 16$ . Figures 1 and 2 present the effect of the number of elements on the wake. The results are presented for  $N_w = 12, 16$ , and  $20$ . Figure 1 presents the effect of  $N_w$  on the geometry of the center and outer streamlines. It can be seen that the center streamline is converged in all cases; the convergence of the outer streamline does not appear to be satisfactory. However, the convergence appears more satisfactory from the way the same results are presented in Fig. 2 which shows the cross section of the wake geometry at four and nine chord lengths behind the trailing edge. It is apparent from Fig. 2 that the solution is essentially converged except for a small region near the outer streamline. This problem is discussed in detail later. Next consider the effect of the number of surface elements along the  $y$  direction ( $N_y$ ) on the convergence of the wake geometry. The cross section of the wake at sixteen chord lengths behind the trailing edge is shown in Fig. 3. The results are obtained for  $N_x = 4$ ,  $N_y = 10, 15, 20$ ,  $\ell_w/c = 16$ , and  $N_w = 16$ . The rate of convergence is very high:  $N_y = 10$  is very close to the converged geometry of the wake.

Next consider the effects of the angle of attack and the aspect ratio on the rolled-up wake geometry. The first is shown in Fig. 4, for a rectangular planar lifting surface of  $AR = 8$ ,  $N_x = 4$ ,  $N_y = 10$ ,  $\ell_w/c = 16$ ,  $N_w = 16$ , at nine chord lengths behind the trailing edge for angles of attack  $\alpha = 5^\circ$ ,

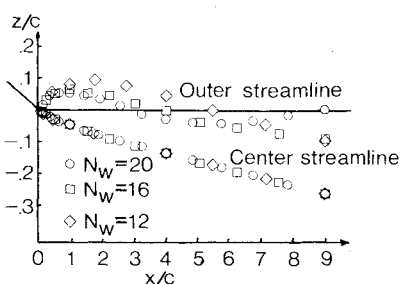


Fig. 1 Convergence analysis: Effect of the number of wake elements on the geometry of center and outer streamlines for a rectangular wing of  $AR = 8$  at  $\alpha = 5^\circ$  ( $N_x = 4$ ,  $N_y = 10$ ,  $\ell_w/c = 16$ , and  $N_w = 12, 16$  and  $20$ ).

$10^\circ$ , and  $15^\circ$ . The results for  $\alpha = 15^\circ$  are mainly of academic interest, since the flow is probably separated at such a high angle of attack. The behavior of the wake is correct from a qualitative point of view. It may be seen that the wake deformation is more pronounced at higher angles of attack. This is to be expected, since the load on the wing is higher at higher angles of attack. The effect of the aspect ratio on the rolled-up

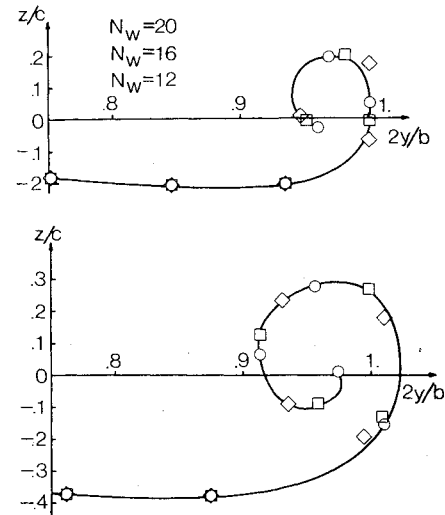


Fig. 2 Convergence analysis: effect of the number of wake elements on the geometry of the wake cross section at  $(x - x_{T.E.})/c = 4$  and  $9$  for a rectangular wing of  $AR = 8$  at  $\alpha = 5^\circ$ ,  $N_x = 4$ ,  $N_y = 10$ ,  $\ell_w/c = 16$ , and  $N_w = 12, 16$  and  $20$ .

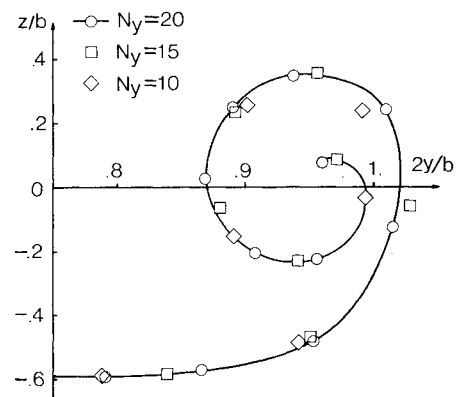


Fig. 3 Convergence analysis: effect on  $N_y$  on the geometry of the wake cross section at  $(x - x_{T.E.})/c = 16$  for a rectangular wing of  $AR = 8$  at  $\alpha = 5^\circ$  ( $N_x = 4$ ,  $N_y = 10, 15$ , and  $20$ ,  $\ell_w/c = 16$  and  $N_w = 16$ ).

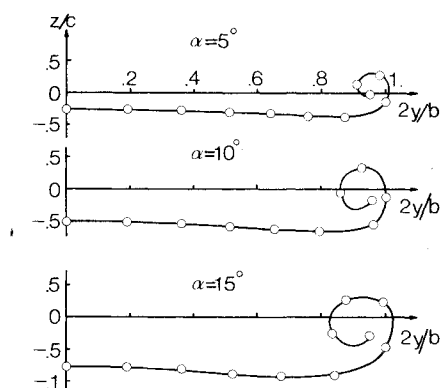


Fig. 4 Effect of the angle of attack on the wake cross section at  $(x - x_{T.E.})/c = 9$  for a rectangular wing of  $AR = 8$  ( $N_x = 4$ ,  $N_y = 10$ ,  $\ell_w/c = 16$ ,  $N_w = 16$ ).

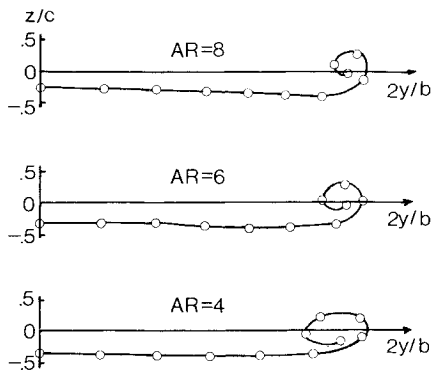


Fig. 5 Effect of the aspect ratio on the wake cross section at  $(x-x_{T,E})/c=9$  for a rectangular wing at  $\alpha=5^\circ$  ( $N_x=4$ ,  $N_y=10$ ,  $\ell_w/c=16$ ,  $N_w=16$ ).

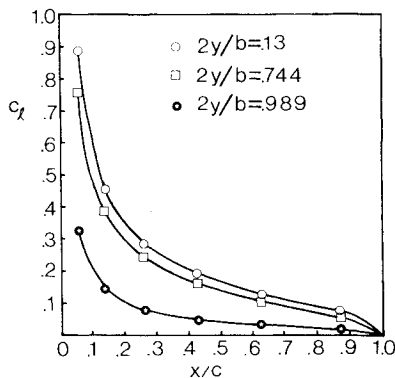


Fig. 6 Lift distribution coefficient at three stations along the semispan for a rectangular wing of  $AR=8$ , at  $\alpha=5^\circ$  ( $N_x=N_y=7$ ,  $\ell_w/c=10.56$ ,  $N_w=13$ ).

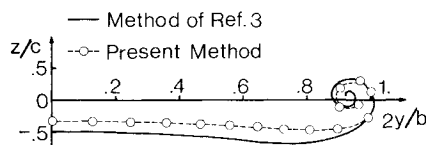


Fig. 7 Wake cross section at  $(x-x_{T,E})/c=9$  and comparison with the theoretical results of Ref. 3 for a rectangular wing of  $AR=8$ , at  $\alpha=6.25^\circ$  ( $N_x=4$ ,  $N_y=15$ ,  $\ell_w/c=10.56$ , and  $N_w=13$ ).

wake geometry is shown in Fig. 5, for rectangular planar lifting surfaces of aspect ratio  $AR=4, 6$ , and  $8$ . The angle of attack is  $5^\circ$  for all three cases,  $N_x=4$ ,  $N_y=10$ ,  $\ell_w/c=16$ ,  $N_w=16$ , and the wake cross sections are situated at nine chord lengths behind the trailing edge. Note that the streamline vertical displacement as well as the tip roll-up is more pronounced for lower-aspect-ratio wings. This might be due to the fact that the velocity induced by the tip vortices is larger in lower-aspect-ratio wings than in higher-aspect-ratio wings (for an infinite-aspect-ratio the induced velocity is zero).

Next consider the effect of the wake deformation on the wing load. Figure 6 shows the lift distribution coefficient at three stations along the wing-span for a rectangular planform of  $AR=8$  at  $\alpha=5^\circ$  angle of attack, with  $N_x=N_y=7$ ,  $N_w=12$ ,  $\ell_w/c=10$ . The calculated lift distribution coefficient is the same (within plotting accuracy) whether the wake is flat or rolled-up (converged), indicating very little wake effect on the wing load. (It should be noted that the effect is expected to be more pronounced for the wing-tail interference, which is one of the ultimate goals of this work.)

Comparison with existing results are presented in Figs. 7-9. Figure 7 presents the wake cross section at nine chord lengths behind the trailing edge for a rectangular lifting surface of aspect ratio  $AR=8$ , at angle of attack  $\alpha=6.25^\circ$ . The results

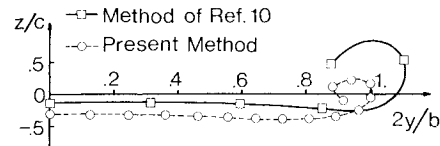


Fig. 8 Wake cross section at  $(x-x_{T,E})/c=4$  and comparison with the theoretical results of Ref. 10 for a rectangular wing of  $AR=6$  at  $\alpha=10^\circ$  ( $N_x=4$ ,  $N_y=15$ ,  $\ell_w/c=10.56$ , and  $N_w=13$ ).

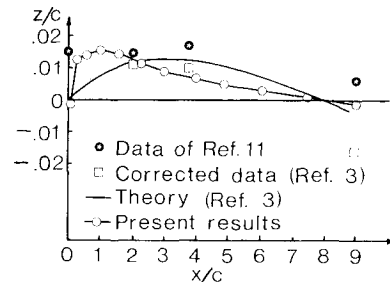


Fig. 9 Location of the vortex centerline and comparison with the results of Refs. 3 and 11 for a rectangular wing of  $AR=6$ , at  $\alpha=12^\circ$  ( $N_x=4$ ,  $N_y=15$ ,  $\ell_w/c=10.56$  and  $N_w=13$ ).

are obtained with  $N_x=4$ ,  $N_y=15$ ,  $\ell_w/c=10.56$ ,  $N_w=13$  and are compared to those of Ref. 3. Excellent agreement is observed in the wing-tip region, while the displacement of the rest of the streamlines is smaller with the present formulation. The present method differs from the one of Ref. 3 because of the inclusion of the effects of the wake deformation on wing loading and the three-dimensionality of the wake geometry. Since the first effect appears to be negligible (see Fig. 6), it seems reasonable to assume that the difference represents the effect the three-dimensionality of the wake geometry. Figure 8 presents the wake cross section at four chord lengths behind the trailing edge for a rectangular lifting surface of aspect ratio  $AR=6$ , at angle of attack  $\alpha=10^\circ$ . The results are obtained with  $N_x=4$ ,  $N_y=15$ ,  $\ell_w/c=10.56$ ,  $N_w=13$  and are compared with those of Ref. 10. The method of Ref. 10 is similar to the present method. The discrepancies in the results of Fig. 8 seem to be due to the fact that more streamlines are used to obtain the present results, especially in the tip-vortex region. A comparison with the results of Refs. 3 and 11 is presented in Fig. 9 which shows the height of the vortex core as a function of  $x$  for a rectangular planar lifting surface with aspect ratio  $AR=6$ , and angle of attack  $\alpha=12^\circ$ . The present results are obtained with  $N_x=4$ ,  $N_y=10$ ,  $\ell_w/c=10.56$ , and  $N_w=13$ . In the method of Ref. 3, as well as in the present method, the vortex core is graphically defined as the center of the tip-vortex spiral while in the experiments of Ref. 11, the vortex core position is defined as the set of points where tangential velocity is zero. In Ref. 3, corrections of the results of Ref. 11 are made, to account for the presence of the wind-tunnel walls. The original and corrected data of Ref. 11 are shown in Fig. 9. The comparison between present and experimental results shows that the tip vortex location obtained with the present method is relatively close to the experimental one, especially at two and four chord lengths behind the trailing edge. (Note that the vertical scale is approximately one hundred times larger than the horizontal one). Note that the original and corrected experimental results bracket both theoretical results shown in Fig. 9. Note also that in both theoretical formulations, the wake emanates from the trailing edge but not from the wing-tip, while in actuality the tip vortex starts at the wing-tip. This is causing the difference between theoretical and experimental results near the trailing edge. The inclusion of the portion of the wake emanating from the wing-tip is now underway. Note also that the method of Ref. 3 is two-dimensional, and this is the possible cause of discrepancy in the comparisons with the present method (as already discussed in the description of the results of Fig. 7).

## V. Discussion and Conclusions

An exact nonlinear integral formulation for lifting surfaces in steady incompressible potential flows has been presented. The formulation treats the wake as a doublet layer. This is a considerable advantage because the wake roll-up procedure is applicable to the general formulation of Refs. 7 and 8 for complex aircraft configurations in steady and unsteady, subsonic and supersonic flows. Applications to windmills and helicopters are also under investigation.

The numerical procedure for the solution of the exact nonlinear formulation is based upon the finite-element technique and is embedded in the computer program ILSA.

The only approximations involved are numerical in nature. No small-perturbation assumption has been invoked. Therefore converged solutions may be considered as exact solutions to the exact nonlinear formulation of the problem. The analysis of convergence indicates that the solution converges very rapidly except for the outer streamline. One possible reason is that, at the wing tip,  $\Delta\phi$  goes to zero like the square root of the distance from the wing tip; therefore the approximation of constant  $\Delta\phi$  might be inappropriate for the outer wake strip. Also the wake is assumed to emanate from the trailing edge. Therefore an improvement is expected by including the portion of the wake emanating from the wing tip. These items deserve further analysis and are now under investigation.

The effects of the angle of attack and of the aspect ratio have been presented. As mentioned previously the ultimate goal of this work is the inclusion of the wake roll-up in the computer program SOUSSA (Steady, Oscillatory and Unsteady, Subsonic and Supersonic Aerodynamics, Ref. 12) for complex aircraft configurations in steady and unsteady, subsonic and supersonic flows. In particular, the wake roll-up is expected to have pronounced effects on the wing-tail interference. The wake-roll-up formulation for complex configurations is presented in Ref. 13. Preliminary results on wake roll-up for thick wings have been obtained.<sup>13</sup>

Comparison with the results of Refs. 3, 10, and 11 indicates that the present results are in good agreement with existing ones. The method is also relatively fast. For instance for the problem of Fig. 6, the solution obtained with ILSA converges (to the fifth figure) in five iterations and requires eight minutes and sixteen seconds on the IBM 370/145 of the Boston University Computing Center. Additional features to accelerate the iteration scheme (such as partial sweeping of the iteration of the wake) are now under consideration.

In conclusion a method for the wake roll-up for lifting surfaces in steady incompressible flows has been developed. The method may be extended to flow analysis around complex configurations in subsonic and supersonic flows as well. Numerical results and comparison with existing ones indicate that the method is not only general and simple, but also accurate and fast.

## Appendix A

All the integrals given in the main body of the paper are evaluated by assuming that the surface elements are quadrilateral and are approximated by a hyperboloidal element introduced in Ref. 7, i.e., by the portion of the hyperboloidal paraboloid

$$P = P_0 + \xi P_1 + \eta P_2 + \xi\eta P_3 \quad (A1)$$

limited by

$$\begin{aligned} -1 \leq \xi \leq 1 \\ -1 \leq \eta \leq 1 \end{aligned} \quad (A2)$$

Introducing the base vectors

$$\begin{aligned} a_1 &= \partial P / \partial \xi = P_1 + \eta P_3 \\ a_2 &= \partial P / \partial \eta = P_2 + \xi P_3 \end{aligned} \quad (A3)$$

the normal is given by

$$n = a_1 \times a_2 / |a_1 \times a_2| \quad (A4)$$

whereas the surface element is given by

$$d\sigma = |a_1 \times a_2| d\xi d\eta \quad (A5)$$

Thus, the integral in Eq. (11) is given by

$$I = \int_{-1}^1 \int_{-1}^1 f(\xi, \eta) d\xi d\eta \quad (A6)$$

where

$$f = \nabla \cdot \frac{\partial}{\partial n} \left( \frac{1}{r} \right) |a_1 \times a_2| \quad (A7)$$

with

$$r = |P - P_h| \quad (A8)$$

Note that, since (Ref. 9)

$$f(\xi, \eta) = \frac{\partial^2 F}{\partial \xi \partial \eta} \quad (A9)$$

where

$$F = \frac{1}{5} (r \cdot a_2 r \times a_2 / |r \times a_2|^2 - r \cdot a_1 r \times a_1 / |r \times a_1|^2) \quad (A10)$$

then

$$I = F(1, 1) - F(1, -1) - F(-1, 1) + F(-1, -1) \quad (A11)$$

Note that  $A_{hk}$  (see Eq. 8) is evaluated by using Eq. (12).

Finally note that the integral over the wake strip is evaluated by approximating the infinite strip with a finite number of quadrilateral hyperboloidal elements, the last of which is one hundred times  $\ell_w$  and parallel to the undisturbed flow.

## References

- Rosow, V. J., "Survey of Computational Methods for Lift-Generated Wakes," *Aerodynamic Analyses Requiring Advanced Computers*, NASA SP-347, Part II, March 1975, pp. 897-923.
- Moore, D. W., "The Discrete Vortex Approximation of a Vortex Sheet," Rep. AFOSR-1084-69, California Institute of Technology, Pasadena, Calif., 1971.
- Bloom, A. M. and Jen, H., "Roll-Up of Aircraft Trailing Vortices Using Artificial Viscosity," *Journal of Aircraft*, Vol. 11, Nov. 1974, pp. 714-716; also unpublished results.
- Maskew, B., "Numerical Lifting Surface Methods for Calculating the Potential Flow About Wings and Wing-Bodies of Arbitrary Geometry," Ph.D. thesis, Loughborough University of Technology, England, Oct. 1972.
- Kandil, O.A., Mook, D.T., and Nayfeh, A.H., "Nonlinear Prediction of the Aerodynamic Loads on Lifting Surfaces," AIAA Paper 74-503, Palo Alto, Calif., 1974.
- Suciu, E.O., "A Finite Element Analysis of the Exact Nonlinear Formulation of a Lifting Surface in Steady Incompressible Flow, with the Evaluation of the Correct Wake Geometry," Master Thesis, Boston University, College of Engineering, Boston, Mass., 1975.
- Morino, L., Chen, L.T., and Suciu, E.O., "Steady and Oscillatory Subsonic and Supersonic Aerodynamics around Complex Configurations," *AIAA Journal*, Vol. 13, March 1975, pp. 368-375.
- Morino, L., "A General Theory of Unsteady Compressible Potential Aerodynamics," NASA CR-2464, Dec. 1974.
- Morino, L. and Suciu, E.O., "A Finite-Element Method for Lifting Surfaces in Steady Incompressible Subsonic Flow," TR-74-05, Boston University, College of Engineering, Department of Aerospace Engineering, Boston, Mass., Dec. 1974.
- Shollenberger, C.A., "A Three-Dimensional Wing/Jet Interaction Analysis Including Jet Distortion Influences," *Journal of Aircraft*, Vol. 12, Sept. 1975, pp. 706-713.
- Chigier, N.A. and Corsiglia, V.R., "Wind-Tunnel Studies of Wing Wake Turbulence," *Journal of Aircraft*, Vol. 9, Dec. 1972, pp. 820-825.
- Tseng, K. and Morino, L., "Fully Unsteady Subsonic and Supersonic Potential Aerodynamics of Complex Aircraft Configurations for Flutter Applications," *Proceedings of AIAA/ASME/SAE 17th Structures, Structural Dynamics, and Materials Conference*, King of Prussia, Pa., May 1976.
- Suciu, E.O. and Morino, L., "A Nonlinear Finite-Element Analysis of Wings in Steady Incompressible Flows with Wake Roll-Up," AIAA Paper 76-74, Washington, D.C., 1976.